Low Water, Tanker Traffic, and Retail Fuel Prices: Evidence from Germany

Johannes Bleher[a,c,*], Konstantin Kuck[b,c]

[a] *University of Hohenheim, Econometrics and Empirical Economics, Schloss Hohenheim 1 C, 70599 Stuttgart, Germany*

[b] *University of Hohenheim, Communication, Information & Media Center, Garbenstrasse 15, 70599 Stuttgart, Germany*

[c] *University of Hohenheim, Computational Science Hub (CSH), Schloss Hohenheim 1 C, 70593 Stuttgart, Germany*

Abstract

Hydrological stress can disrupt freight transport, but downstream retail-price consequences are harder to identify. We study fuel logistics using high-frequency retail prices, river gauges, AIS tanker movements, road counts, and infrastructure geography. Mixed-threshold low-water stress is associated with fewer tanker crossings and lower average speed among observed crossings, although count precision is marginal under waterway-and-date clustering. German net diesel-price changes co-move positively with low-water breadth and depth relative to fixed European controls, but placebo tests leave this comparison descriptive. Regional price gradients by baseline tanker dependence are mixed and statistically unresolved under federal-state-by-date fixed effects. Secondary spatial-dispersion and intraday-variability outcomes do not survive multiplicity adjustment. The regional event study rejects the joint no-pretrend restriction, and river exclusions matter. Evidence is therefore stronger for a low-water association with tanker movement than for downstream prices; it identifies neither a causal national price effect nor the domestic or cross-border adjustment mechanism.

Keywords: Inland waterways; fuel prices; hydrological extremes; transport infrastructure; climate adaptation; supply-chain resilience; Germany
JEL Classification: Q54; Q41; R41; L91; H54

[*] Corresponding author. Tel.: +49 711 459 23054
Email addresses: johannes.bleher@uni-hohenheim.de (Johannes Bleher), konstantin.kuck@uni-hohenheim.de (Konstantin Kuck)

1. Introduction

Environmental shocks to freight systems can propagate beyond transport when they constrain the movement of essential inputs and goods. Inland waterways are particularly exposed because navigability depends directly on hydrological conditions, while inventories, terminals, and alternative modes may buffer downstream markets. Exceptionally low or high water can reduce payloads, force detours, delay shipments, or temporarily close routes. Whether such physical disruption produces broader market effects is therefore a transport-resilience question as well as an environmental one. Germany provides an informative setting: its inland-waterway network connects industrial production sites, inland refineries, storage facilities, and seaports and carries bulk commodities and refined petroleum products along the Rhine and its tributaries, the Danube, the Weser, Elbe, and Oder systems, and connecting canals.[1]

This issue has become increasingly relevant in recent years. A prominent example is 2022, when inland-waterway freight volumes in Germany fell by 6% relative to the previous year, partly attributed to low water in August (Statistisches Bundesamt, 2023). More broadly, climate change is expected to alter discharge patterns, drought frequency, and flood risks, with potentially important implications for European inland navigation (Christodoulou et al., 2020). The central economic question is therefore not only whether low water interrupts shipping. It is whether a transport disruption is transmitted to consumers or absorbed by inventories, terminals, substitute modes, and other supply-chain buffers.

This paper studies this supply-chain resilience margin in German fuel markets. Fuel is a particularly informative setting for three reasons. First, refined petroleum products account for a meaningful share of inland-waterway freight.[2] Second, retail fuel prices are observed at high frequency and display rapid adjustment, making them a useful downstream indicator of transport disruptions. Third, the German fuel market exhibits broad geographic coverage and multiple potential supply margins, allowing us to study how a shock in one waterway corridor is absorbed or transmitted across space rather than only at a single bottleneck. Germany is also embedded in a wider European product market. Cross-border procurement could replace supply impaired on a domestic waterway, but the available data do not identify whether this adjustment occurs.

Empirically, we combine high-frequency station-level fuel prices from tankerkoenig.de (2025) with river-gauge information from Wasserstraßen- und Schifffahrtsverwaltung des Bundes (WSV) (2025), spatial information on river-basin districts Bundesanstalt für Gewässerkunde (BfG) (2025), and a national grid that maps stations and hydrological exposure into a common spatial framework. We then estimate how river-specific low-water, high-water, and non-navigable conditions are associated with diesel, E5, and E10 prices across German grid cells over time. Our price estimates should be interpreted as reduced-form retail-price gradients. They summarize differential retail-price movements and do not separately identify inland-waterway supply constraints, substitution, inventories, or other adjustment margins.

The main empirical finding is deliberately asymmetric. The results separate three estimands. Mixed-threshold low water is associated with fewer crossings and lower average speed among observed crossings,

[1] See Eurostat (2025) for further details about the goods transported on inland waterways in 2023.
[2] See Eurostat (2025) for further details about the goods transported on inland waterways in 2023.

but crossing-count precision weakens when inference is conducted at the waterway level. National low-water breadth and depth are positively associated with German net diesel-price changes relative to fixed EU controls, although placebo evidence does not identify a causal national effect. The post-June-2021 regional design finds no stable differential response by baseline tanker dependence once state-day shocks and multiplicity are addressed. Secondary spatial-dispersion and intraday-variability estimates are also statistically unresolved after Holm adjustment. Baseline AIS exposure is a proxy for tanker dependence, not a complete vulnerability measure; storage, terminals, pipelines, inventories, alternative modes, and cross-border sourcing remain unobserved candidate mechanisms rather than explanations identified by the price regressions. The main result is therefore an asymmetry in evidentiary strength, not a proven divergence in causal effects.

A separate national comparison finds positive weekly German net-price changes relative to synthetic EU controls and a four-week buildup, but weak country-placebo ranks and reversal by eight weeks preclude a strong causal interpretation.

The policy implication is narrower than a ranking of adaptation measures. The evidence motivates evaluating waterway operations and supply-chain contingency jointly, but it does not estimate the benefits of forecasting, fairway investment, storage, terminal capacity, modal substitution, or cross-border sourcing. German policy already provides operational probabilistic water-level forecasts and is advancing targeted fairway optimization at Middle Rhine bottlenecks (Bundesministerium für Verkehr, 2024, 2025). These are policy responses against which the paper's transport evidence is relevant, not interventions evaluated by the present design.

The paper contributes by placing a direct tanker-movement diagnostic beside national and regional retail-price estimands without forcing them into a single pass-through parameter. Christodoulou et al. (2020) study climate risk for inland navigation, while Jonkeren et al. (2007) quantify Rhine low-water transport costs. Recent evidence is closer to our setting. Bedoya-Maya et al. (2024) estimate throughput losses from critical Rhine water levels, and Pulido et al. (2025) link daily waterway events to vessel passages across the Rhine–Main–Danube network. The latest version of Horst and Müller (2025) reports regional economic effects, energy-market price responses, and substitution toward suppliers less reliant on Rhine transport. Relative to that work, our narrower contribution is the combination of high-frequency German pump prices, AIS tanker crossings, and an explicit separation between descriptive national co-movement and within-state daily price gradients. The results motivate supply-network adjustment as a research question but do not identify a European or domestic buffer.

The paper also treats transport-channel evidence separately from the price regressions. The price design identifies whether hydrological shocks are associated with differential fuel-price movements, but it does not directly observe the transport channels through which these movements operate. Three additional data sources are therefore used to discipline the interpretation. Vessel-level AIS data measure whether tanker traffic falls in exposed river corridors when water levels become extreme. BASt road-count data test whether nearby truck traffic rises on substitution corridors or falls around inland-harbor catchments when navigation is impaired. Pipeline geodata measure whether areas with stronger potential pipeline access are less sensitive to river disruptions. Taken together, these layers allow the reduced-form price estimates to be interpreted against a more explicit transport mechanism.

The remainder of this paper is structured as follows. Section 2 presents the data and methodology, Section 3 reports the empirical results, Section 4 discusses interpretation and limitations, and Section 5 concludes.

2. Data and Empirical Strategy

2.1. Data Sources

The empirical analysis draws on ten main data sources. First, retail fuel prices and station metadata come from the historical data of tankerkoenig.de (2025). Weekly national diesel and Euro 95 prices with and without taxes, together with VAT, excise-duty, and other-indirect-tax series, come from the European Commission's Weekly Oil Bulletin (European Commission, 2026). Second, hydrological information on German gauge stations and daily water levels comes from Wasserstraßen- und Schifffahrtsverwaltung des Bundes (WSV) (2025). Third, river-basin boundaries are obtained from Bundesanstalt für Gewässerkunde (BfG) (2025). These sources underpin the reduced-form price analyses. To study mechanism, we additionally use vessel-level AIS data from the Kpler archive of inland-waterway traffic in Germany and the Danube, hourly BASt road-count data for autobahns and federal roads, and pipeline geodata derived from OpenStreetMap-based infrastructure extracts. Conceptually, AIS measures realized shipping activity, BASt tests for observable road-freight substitution, and pipeline data measure potential alternative transport infrastructure. Three public sources sharpen the supply-side diagnostics: German port-to-port inland-shipping records for liquid petroleum products (Statistische Ämter des Bundes und der Länder, 2026), Eurostat monthly road-diesel deliveries, imports, and emergency stocks (Eurostat, 2026), and member-site nameplate storage capacity reported by the German independent tank-storage association (Unabhängiger Tanklagerverband e.V., 2025). The first two are national monthly series and the third is a 2025 cross-section; they are therefore used as mechanism and heterogeneity evidence rather than controls in the preferred daily price model. The Eurostat balance reports total German imports but not bilateral partner countries or the transport route by which imported product enters Germany.

2.2. Panel Construction

The analytic dataset combines high-frequency fuel prices, hydrological information, and spatial transport exposure data in a common daily panel.[3] We begin with the historical station-level fuel data of tankerkoenig.de (2025). For each gas station and day, we compute daily summary measures for diesel, E5, and E10 and retain the daily mean price as the main target variable. The event log is reconstructed chronologically: strictly positive values contribute to time-weighted prices, whereas nonpositive sentinel values mark a product as unavailable and never enter a price average. We retain the duration and incidence of product-specific unavailability separately from all-fuel station unavailability, so that possible scarcity at the extensive margin can be tested without treating a status code as a price. Station metadata provide a unique identifier and geographic coordinates, which allow each station to be assigned to a specific cell in a common spatial grid. Dated Tankerkönig station snapshots begin in 2019. Earlier price observations are mapped using the first observed coordinates for the same station identifier. This backward coordinate carry affects the historical descriptive

[3] A detailed documentation of the dataset construction in terms of R code is available on request.

panel, but the internally frozen regional price design begins on July 1, 2021, and therefore does not rely on pre-snapshot location backcasting. The empirical analysis is conducted at the level of grid cells rather than individual stations in order to align retail prices with river, road, and pipeline exposure measures. The grid is constructed as a system of 50-kilometer cells covering Germany in an azimuthal equidistant projection centered on Stuttgart; grid centroids are stored in longitude and latitude for subsequent matching.

Table 1: Analysis-sample coverage of analytic time series and panels

The table reports temporal coverage and observation levels within the analysis samples used in the price, hydrological, AIS, BASt, weather, and public freight exercises. Hydrological and public-freight rows are restricted to the fuel-price analysis window where applicable; AIS and BASt rows report their mechanism-analysis windows. The source-wide panels cover longer or differently defined windows, while raw moments and static infrastructure summaries preserve information deliberately omitted from this analysis-sample table. For details, see Appendix Tables B.1, B.2, and B.3.

Series	Frequency	Unit level	Start	End	Periods	Obs.
Diesel price	Daily	Grid-day	2014-06-09	2026-06-30	4,405	788,453
E5 price	Daily	Grid-day	2014-06-09	2026-06-30	4,405	787,819
E10 price	Daily	Grid-day	2014-06-09	2026-06-30	4,405	785,486
Standardized water level	Daily	Gauge-day	2014-06-08	2026-06-30	4,406	2,336,456
Low-water navigation constraint	Daily	River-day	2014-06-08	2026-06-30	4,406	39,654
Low-water depth deficit	Daily	River-day	2014-06-08	2026-06-30	4,406	39,654
High-water navigation restriction	Daily	River-day	2014-06-08	2026-06-30	4,406	39,654
High-water closure state	Daily	River-day	2014-06-08	2026-06-30	4,406	39,654
Precipitation	Daily	Grid-day	2014-06-08	2026-06-30	4,406	788,631
Temperature	Daily	Grid-day	2014-06-08	2026-06-30	4,406	788,631
AIS tanker vessels	Daily	River-day	2021-01-01	2022-11-30	689	4,059
AIS tanker messages	Daily	River-day	2021-01-01	2022-11-30	689	4,059
AIS tanker crossings	Daily	Gate-direction-day	2021-01-01	2022-11-30	687	58,715
BASt truck traffic	Daily	Station-day	2021-01-01	2022-12-31	730	1,211,435
BASt heavy-vehicle traffic	Daily	Station-day	2021-01-01	2022-12-31	730	1,148,655
Rail refined-petroleum freight	Monthly	National month	2014-06-01	2026-04-01	143	143
Inland-waterway refined-petroleum freight	Monthly	National month	2014-06-01	2026-03-01	142	142
Rail share in rail-waterway petroleum freight	Monthly	National month	2014-06-01	2026-03-01	142	142
Official low-water gauge-day share	Monthly	National month	2014-06-01	2026-04-01	143	143

Hydrological data are assembled from the gauge network provided by Wasserstraßen- und Schifffahrtsverwaltung des Bundes (WSV) (2025). For each station, we retrieve gauge identifiers, locations, daily water-level readings, and official characteristic values. The preferred event measures are navigation-relevant rather than purely hydrological: low-water navigation constraints use the equivalent water level (GlW) or equivalent navigation reference values where available; high-water navigation restrictions use official high-water marks; and high-water closure risk uses the highest navigable water level (HSW). As fallback and for robustness checks we retain MNW for low water and station-specific empirical percentiles where an operative navigation threshold is unavailable. Empirical fallback thresholds and gauge standardization are calibrated once on 2000–2013 observations and require at least 365 valid reference days per gauge; extending the dataset therefore does not reclassify earlier events. There is no symmetric official low-water closure threshold in these data. We therefore measure low-water severity continuously as meters below the operative GlW/RNW or fallback threshold rather than creating an artificial closure category. High-water severity is measured symmetrically as meters above the operative restriction threshold, while HSW remains a separate institutional closure threshold. The pipeline respects each characteristic value's official validity date and does not apply a current GlW retrospectively. Major Rhine GlW values in the current API are valid from 2023, so earlier low-water episodes, including 2018 and 2022, are classified using the stated fallback rules unless a historically valid official value is available. For the navigation-event construction, exact zero readings are treated as missing only when they are more than one meter and ten station-specific median absolute deviations from the station median; 339 gauge-days meet this rule. Five isolated extreme negative readings are also removed when they lie more than both five meters and twenty median absolute deviations below the station median. Before applying either sentinel rule, an annual-median scale check excludes four gauges with more than tenfold unit breaks from fallback calibration and event construction. River-day reporting shares use gauges whose own first-to-last valid observation span includes the date; retired and not-yet-active gauges remain in the audit count but do not create artificial daily nonresponse. The excluded gauges and sentinel counts are reported in Appendix Table F.2. Table 2 summarizes the event taxonomy, and Table 3 reports threshold coverage by river basin. The baseline price panel is obtained by merging grid-day fuel prices with river-basin-day shares of gauges in each navigation-event state.

The GDWS defines GlW as a low-water level reached or undershot on 20 ice-free days per year on average and states that low water does not trigger an administrative navigation ban (Generaldirektion Wasserstraßen und Schifffahrt, 2023). Available fairway depth changes one-for-one with the gauge deviation from GlW. The recommended 30 cm Flottwasser is a safety clearance subtracted from current fairway depth when determining maximum vessel draught; it is not a 30 cm dead zone below GlW. Economic adjustment may nevertheless be delayed by spare draught, partial loading, inventories, or forecasts. We therefore report both gauge-standardized deficits and raw-depth hinge models with assumed operational buffers rather than imposing one institutional cutoff.

Table 2: Navigation-event definitions used in the preferred specifications

The event taxonomy separates entry into a persistent navigation-restriction state from continuous severity beyond the operative threshold. High-water closure risk marks the additional HSW threshold and is not a substitute for the continuous high-water excess measure. Official characteristic values are used only during their documented validity periods.

Event	Preferred threshold	Robustness fallback
Low-water navigation constraint	GlW or RNW	MNW / 2000–2013 station bottom 2%
Low-water depth deficit	Meters below operative low-water threshold	Same fallback hierarchy
High-water navigation restriction	Marke I, II, or III	2000–2013 station top 2%
High-water excess	Meters above operative high-water threshold	Same fallback hierarchy
High-water closure risk	HSW	2000–2013 station top 1%

Table 3: Navigation-threshold coverage by river basin

Entries report the share of PEGEL gauges in each river basin with official navigation or hydrological threshold values in the PEGELONLINE characteristic-value API. GlW/RNW and high-water marks are the preferred navigation thresholds; MNW/MHW are retained for robustness and fallback definitions.

River	Gauges	GlW/RNW	Marke	HSW	MNW	MHW
Donau	19	47.4	0.0	42.1	68.4	68.4
Eider	16	0.0	0.0	0.0	18.8	18.8
Elbe	300	0.0	0.0	4.0	60.7	61.0
Ems	37	0.0	0.0	5.4	29.7	29.7
Oder	32	0.0	18.8	21.9	100.0	100.0
Rhein	165	10.9	22.4	33.9	32.1	31.5
Schlei/Trave	18	0.0	0.0	0.0	88.9	88.9
Warnow/Peene	27	0.0	0.0	0.0	96.3	96.3
Weser	105	5.7	23.8	22.9	35.2	35.2

To trace transport adjustment during hydrological stress, we assemble three additional datasets. First, vessel-level AIS data are aggregated to daily river-basin panels in order to measure realized shipping activity, especially tanker traffic, along exposed inland-waterway corridors. Second, hourly BASt road-count data are aggregated to daily station-, road-, and corridor-level panels, which allows us to test whether truck traffic rises when inland navigation becomes more difficult. Third, pipeline geodata are mapped to the same spatial grid as the fuel-price data, yielding measures of pipeline presence, proximity, and potential access to pipeline network nodes. As a cautious supply-network diagnostic, the pipeline also constructs an OpenStreetMap (OSM) derived petroleum supply-node layer from oil-like pipeline endpoints and junctions. This layer is used for matching and descriptive validation only; it is not treated as a preferred causal exposure because OSM tagging and coverage are incomplete. The preferred spatial measure is baseline AIS tanker dependence: river-specific crossing activity in January–June 2021, distance-weighted to each price grid. Harbor proximity, pipeline access, and public supply nodes are retained as separate adjustment and balance variables. A weighted composite that mixes AIS dependence with these buffers is reported only as a sensitivity check because its components have different causal roles and its low-water coefficient reverses sign. These transport layers are not introduced as generic controls; rather, they are used to discipline the interpretation of the reduced-form estimates by tracing disruption, substitution, and resilience.

2.3. Retail-Price-Gradient Model

The preferred price model asks whether navigation stress is associated with differential price movements in markets with greater predetermined tanker dependence. Let y_{it} denote log price in grid cell i on date t, let $\mathbf{H}_{rt}$ collect low-water restriction and depth, high-water restriction and excess, and the HSW closure-threshold indicator for river r, and let D_{ir} denote standardized baseline AIS tanker dependence. We estimate

$$y_{it} = \sum_{r} \mathbf{H}'_{rt} \boldsymbol{\beta} D_{ir} + \mathbf{Z}'_{it} \boldsymbol{\gamma} + \mu_i + \lambda_{s(i)t} + \varepsilon_{it}. \tag{1}$$

Here μ_i are grid fixed effects, $\lambda_{s(i)t}$ are federal-state-by-date fixed effects, and $\mathbf{Z}_{it}$ contains DWD precipitation and temperature controls. Grid fixed effects absorb stable local price, income, demand, and market-structure levels. Federal-state-by-date fixed effects absorb daily wholesale, tax, macroeconomic, calendar, and supply shocks shared within each state; the less restrictive grid-and-national-date model remains a benchmark. Explicit holiday and school-vacation interactions provide a named-calendar sensitivity. For details, see Appendix Table A.9. The preferred model excludes lagged prices because persistent, anticipated hydrological stress may already affect the lag. For details, see Appendix Table A.15.

Date fixed effects absorb the national main effect of the 2022 German fuel-tax cut, but not heterogeneous pass-through correlated with tanker dependence. Adding the statutory tax-cut window interacted with standardized total baseline AIS dependence barely changes the low-water estimates. This is a targeted sensitivity check rather than part of the preferred specification. For details, see Appendix Table A.10.

Identification comes from comparisons of grids with different pre-event tanker dependence within the same federal state and date. The outcome window begins on July 1, 2021, after the January–June 2021 AIS baseline is measured. Coefficients are reduced-form differential price gradients, not national price effects or structural transport elasticities. Standard errors are two-way clustered by grid and date. Retail price levels remain the primary outcomes because they measure consumer-facing pass-through. As secondary market-stress outcomes, we estimate (i) the grid-day interquartile range of station-level daily mean prices, (ii) the grid-day median of station-level time-weighted intraday price standard deviations, and (iii) the grid-day median of station-level event-based realized price variation, $\sqrt{\sum_j (\Delta p_{jsd})^2}$. The event measure uses chronologically reconstructed price changes within station s and day d; it includes only genuine price-change messages with strictly positive prices before and after the event and excludes product removal and re-entry. All outcomes require at least three observed stations with at least 80 percent known daily price-state coverage. They are estimated in euro-per-liter levels using the same mixed-threshold hydrological terms, grid and federal-state-by-date fixed effects, DWD controls, and two-way clustering as Equation (6). We report effects in cents per liter and apply a joint Holm correction across the nine fuel-by-outcome tests. These measures capture realized dispersion or repricing, not expectations or uncertainty.

2.4. National and Relative Price Outcomes

Equation (6) cannot identify a national hydrological price response because date fixed effects absorb every price movement shared by German grids. We therefore separate a national weekly estimand from the regional daily gradient. For fuel f, country c, and week t, let P_{fct} denote the Weekly Oil Bulletin price and define the German price gap

$$g_{ft} = 100 \left[\log P_{f,\mathrm{DE},t} - \sum_{c \in \mathcal{C}} w_{fc} \log P_{fct} \right]. \tag{2}$$

The nonnegative weights w_{fc} sum to one and minimize the discrepancy in weekly net-of-tax log-price changes during January 2009–December 2013. The donor pool comprises Cyprus, Denmark, Estonia, Spain, Finland, Greece, Ireland, Italy, Lithuania, Latvia, Malta, Poland, Portugal, and Sweden; countries on the main Rhine and Danube corridors are excluded. The weights are fixed for the June 2014–June 2026 analysis window, and the net-price weights are also applied to tax-inclusive prices. In each fuel design, only a small subset of donor countries receives positive weight. For details, see Appendix Table A.13.

National hydrological stress is aggregated with equal, fixed weights across the Rhine, Elbe, Weser, and Danube. The breadth measure is the weighted share of these major corridors in a persistent low-water state; the depth measure is their weighted distance below the operative threshold. January–June 2021 AIS tanker weights are retained only as a sensitivity analysis because using them for earlier outcomes would import future network information. Breadth and depth enter separate regressions of Δg_{ft} with year and calendar-month fixed effects. Inference uses Bartlett heteroskedasticity-and-autocorrelation-consistent standard errors with eight weekly lags, with 4, 13, and 26 lags as sensitivities. Donor-country and season-preserving time-shift placebos probe Germany-specific confounding; the estimates remain descriptive rather than synthetic-control causal effects.

For dynamics, the national outcome is $g_{f,t+h} - g_{f,t-1}$ for horizons of zero, one, two, four, and eight weeks. The regional analogue is $\log p_{i,t+h} - \log p_{i,t-1}$ for horizons through 28 days, estimated with the same hydrological interactions, weather controls, grid fixed effects, federal-state-by-date fixed effects, and grid-and-date clustered standard errors as the static model. These regional estimates condition on hydrological stress at date t; they are not clean-onset event studies. Finally, replacing $\log p_{it}$ by $\log p_{it} - \overline{\log p}_t$ in the less restrictive national-date benchmark leaves every event-by-dependence coefficient unchanged up to numerical precision. This verifies that those benchmark coefficients are explicitly relative German price gradients rather than national price effects.

2.5. Conceptual Framework

Figure 1: Causal objects in hydrological disruption and local fuel prices

Solid arrows represent causal pathways; dashed arrows and boxes identify the observed threshold and AIS proxies. The graph separates three objects: forecastable hydrological stress can induce adjustment before actual navigability deteriorates; actual navigability causes disruption conditional on baseline dependence; and $L_{rt}D_{ir}$ is the empirical proxy. Because date fixed effects absorb common event responses, the price equation identifies a differential same-date gradient, not the national episode effect including anticipation or the national average effect of realized navigability. DWD controls address weather-to-demand and weather-to-anticipatory-adjustment backdoor paths, grid fixed effects absorb additive paths from stable local traits, and date fixed effects absorb national wholesale, tax, macroeconomic, calendar, and seasonal shocks. National shocks are outcome determinants, not part of the minimal backdoor set in the displayed graph. Correlated regional day shocks remain a threat. Delivered marginal cost is a price mediator; local product availability is a parallel scarcity outcome. Neither is controlled in the price equation. Domestic and cross-border supply capacity is an effect modifier.

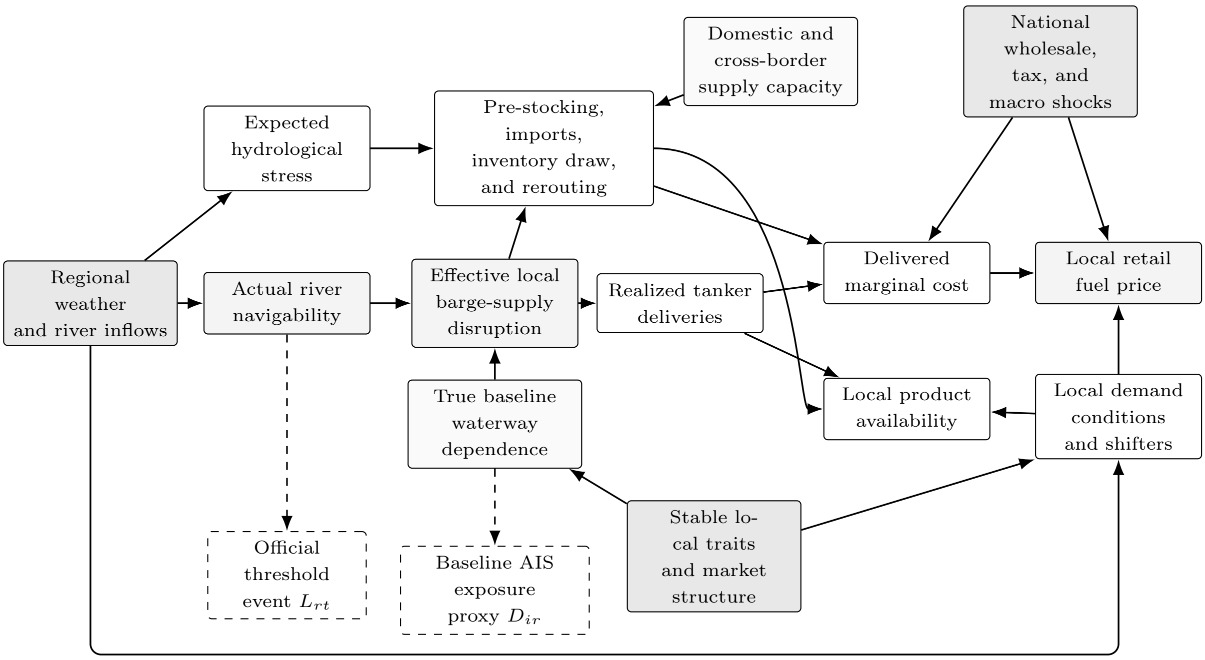

The empirical design is motivated by a simple transport-cost framework rather than by a representative-agent model. Consider a local fuel market i that can be supplied through geographic sources $s \in \mathcal{S}$ and transport modes $m \in \{\text{barge}, \text{truck}, \text{rail}, \text{pipeline}\}$. Let the delivered marginal cost of supplying market i on day t through source-mode combination (s, m) be

$$c_{ismt} = w_{st} + \tau_{ismt}(H_t) + \kappa_{ism}, \tag{3}$$

where w_{st} is the upstream product cost at source s, $\tau_{ismt}(H_t)$ is the source-route transport cost that depends on hydrological conditions H_t, and κ_{ism} captures time-invariant source, route, and infrastructure characteristics. Suppliers allocate shipments across source-mode combinations to minimize delivered cost subject to modal capacity constraints. In the absence of binding constraints, the relevant supply cost for market i is

$$C_{it} = \min_{s,m} c_{ismt}. \tag{4}$$

Retail fuel prices then satisfy

$$p_{it} = C_{it} + T_t + m_{it}, \tag{5}$$

where T_t denotes common fuel taxes and m_{it} is the local retail markup shaped by demand conditions and competition. This notation separates national tax changes, absorbed by date fixed effects, from local price-setting conditions. European market integration expands the feasible set $\mathcal{S}$ rather than constituting a separate transport mode. A river disruption can therefore induce adjustment through another mode, another geographic source, or both.

Hydrological shocks matter because they change the feasibility and cost of inland-waterway transport. Let H_t summarize low-water, high-water, or non-navigable states on a river reach. When river conditions deteriorate, barge transport becomes more expensive because vessels must reduce load factors, face longer travel times, or stop operating altogether. In the notation above, this implies an increase in $\tau_{i,\text{barge},t}(H_t)$ and, in the case of severe disruption, a tightening of effective barge capacity. Freight is then reallocated toward road haulage or pipelines where those margins are available.

This framework yields four empirical implications that map directly into the analysis. First, adverse river conditions should reduce observed vessel traffic on exposed reaches. Second, truck traffic may rise on substitution corridors when barge transport becomes less attractive, but it may also fall near inland harbors if fewer vessels arrive and depart. Third, retail fuel prices may rise more in places that are truly dependent on disrupted waterways and lack buffers. The preferred AIS measure approximates baseline dependence, while harbor, pipeline, public supply access, and access to alternative geographic sources are kept conceptually separate because they may buffer the same shock. A negative event-by-dependence coefficient means that prices moved less in more AIS-dependent grids on the same date; it does not imply that the disruption reduced the national price level. Fourth, price responses should be attenuated where alternative infrastructure or sourcing provides an effective fallback option, although observing a pipeline or harbor nearby is only a coarse proxy for actual usable capacity. Because low water is forecastable, suppliers may also pre-stock, draw inventories, import product, or reroute before the threshold is crossed. These are treatment pathways, not baseline controls, and they motivate the pre-event and public-supply diagnostics. The role of the transport and supply data is therefore not to serve as a generic control block, but to test whether the reduced-form price responses are consistent with an integrated supply problem in which dependence and resilience are spatially correlated.

2.6. Mechanism Design

The transport datasets are used in a second step to evaluate mechanism rather than to saturate the baseline price regression. The AIS reach-day panel is used to estimate whether extreme water levels reduce realized tanker activity on exposed waterways. The BASt panel is used to test whether observable road traffic rises on nearby substitution corridors or falls around inland-harbor catchments when river navigation becomes more difficult. The pipeline data are used to construct cross-sectional exposure measures and to test whether price responses are weaker in grid cells with stronger potential alternative infrastructure. This sequence of baseline and mechanism regressions is central to the interpretation of the results: the fuel-price model documents differential retail-price movements, while the transport panels are used to assess whether those movements are consistent with shipping disruption, road substitution, and infrastructure-based resilience.

In practical terms, the mechanism analysis is concerned with three complementary questions. First, does hydrological stress reduce observed tanker activity on the affected river reach? Second, do road-freight measures such as truck counts and heavy-vehicle shares rise on nearby corridors, or fall around inland-harbor catchments, when river navigation is impaired? Third, are fuel-price responses weaker in locations with stronger potential pipeline access or stronger multimodal substitution capacity? These questions correspond to three empirical objects: a reach-day AIS panel, a corridor-day BASt panel, and grid-level infrastructure exposure measures. Together they allow the paper to move from reduced-form price gradients to a more explicit account of transport disruption, substitution, and buffering.

2.7. Identification Strategy

The transport estimand asks whether persistent navigation stress reduces realized tanker movement at gauge-centered crossing gates; the threshold-source split then determines whether official or fallback episodes provide the identifying variation. The retail-price estimand is the differential same-date diesel, E5, or E10 price gradient during a persistent mixed-threshold low-water constraint for a one-standard-deviation increase in predetermined baseline AIS tanker dependence. Let L_{rt}^{M} combine historically valid official navigation thresholds with the frozen fallback hierarchy on river corridor r and date t, and let D_{ir} denote grid cell i's standardized baseline AIS dependence on that corridor. Official-only estimates are source-support diagnostics rather than substitutes for this primary treatment. Observable buffers are examined in separate heterogeneity designs. The main price specification is

$$\log p_{it}^{f} = \theta^{f} \sum_{r} L_{rt}^{M} D_{ir} + \mathbf{Z}_{it}' \gamma^{f} + \mu_i + \lambda_{s(i)t} + \varepsilon_{it}^{f}, \tag{6}$$

where f indexes the fuel type, μ_i are grid fixed effects, $\lambda_{s(i)t}$ are federal-state-by-date fixed effects, and $\mathbf{Z}_{it}$ contains DWD weather controls. Event main effects shared within a federal state and date are absorbed by $\lambda_{s(i)t}$, and AIS-dependence main effects are absorbed by grid fixed effects. The identifying variation therefore compares more- and less-AIS-dependent grids within the same federal state and date during mixed-threshold low-water constraints. A positive θ^{f} means that prices are higher in relatively more dependent grids on those dates; a negative θ^{f} means that they are lower. It is a differential price gradient, not the frequency of a retail event and not the national average effect of low water. The phrase "total response" is therefore reserved for a precisely defined causal object. The total effect of an anticipated hydrological episode starts when credible forecasts alter inventories and routing; the total effect of realized navigability begins at the realized navigation state and therefore excludes earlier anticipatory responses by definition. Equation (6) identifies neither national effect because $\lambda_{s(i)t}$ absorbs its common state-day component. It leaves downstream deliveries, adjustment, and delivered marginal cost uncontrolled, so θ^{f} is total only with respect to those mediating pathways within the narrower differential-gradient estimand.

The identifying assumption is that, absent mixed-threshold low-water constraints, more- and less-AIS-dependent grids would not have different fuel-price movements on those dates after grid fixed effects, federal-state-by-date fixed effects, and weather controls. Baseline AIS dependence is predetermined from January–June 2021 tanker crossings and does not use fuel-price outcomes. The assumption can still fail if local daily demand or supply shocks are correlated with both event-river dependence and prices. Preferred-specification timing placebos, river exclusions, and exposure permutations probe this threat but do not transform the gradient into a causal estimate.

The river-specific treatment is driven by only nine distinct river histories. Conventional grid-and-date-clustered p-values are therefore reported together with leave-one-river-out sensitivity and are not interpreted as many-shock asymptotics.

Prices enter the preferred specifications in logarithms rather than as a separately normalized price index. A national daily fuel-price index, common deflator, or normalization to a base date would be absorbed by the date fixed effects and therefore would not change the event-by-exposure coefficient. Constructing grid-specific indices would add an arbitrary base-period choice without resolving the identifying challenge. We consequently report log-price gradients and translate selected estimates into cents per liter.

The main threats are regional demand shocks, industrial and infrastructure geography, anticipation and inventory behavior, and measurement error in navigation constraints and dependence. The empirical package addresses these threats in several ways. Placebo-date and wrong-river tests ask whether the result appears on dates or corridors that should not be treated. Broad-region-by-date fixed effects compare more- and less-dependent grids within the same broad region on each date, thereby absorbing region-specific daily demand and supply shocks. Federal-state-by-date fixed effects provide a stronger calendar and regional-shock diagnostic while preserving the grid as the price and observation unit. Additional interactions test whether baseline prices, pipeline access, or inland-harbor proximity change the low-water gradient. Exposure-validity checks report correlations and baseline balance and compare the true estimate with within-region permutations of river-specific AIS dependence. Event-study diagnostics reveal whether differential price movements precede threshold crossing. AIS crossing regressions provide a first-stage association between persistent navigation stress and tanker movement. In the corrected source split, fallback low-water episodes are associated with 5.0 percent fewer crossings, while the official coefficient is near zero and imprecise because official support is confined to two nearly inactive Danube gates. Baseline AIS exposure is nevertheless the preferred price-gradient modifier because it measures the dependence channel directly; the paper does not interpret it as random assignment or as a complete measure of local vulnerability. High-water and closure-state estimates are auxiliary disruption evidence rather than the main causal claim.

The calendar and regional-shock checks answer different questions. Explicit federal-state holiday, adjacent-day, and school-vacation controls test named calendar explanations directly; federal-state-by-date fixed effects additionally absorb all unobserved shocks shared within a state on a date and therefore alter the identifying comparison more broadly.

Baseline income is not a separate node in Figure 1 because its stable effect on local demand is part of the time-invariant local traits absorbed by grid fixed effects. This does not control an income-specific response to low water. Such heterogeneity would require a pre-specified event-by-income interaction, but it is not required to estimate the stated AIS-dependence gradient unless income generates differential daily shocks correlated with river dependence. The broad-region-by-date and federal-state-by-date models are the available diagnostics for that more general threat.

The design does not identify structural transport-cost incidence, shipment-route elasticities, or the marginal cost of barge capacity. It identifies differential retail-price movements during official low-water constraints across markets with different predetermined AIS tanker dependence. Pairing each event with another corridor's AIS-dependence score produces nonzero estimates, showing that river-specific dependence shares broad spatial structure and does not provide perfectly isolated treatments. For details, see Appendix Table A.6. The matched design in Table 8 is therefore a guardrail around the same narrow estimand. A zero or negative gradient is not evidence that disruption lowers the national price level; it means only that prices in more AIS-dependent grids did not rise more than prices in comparison grids.

An event-specific monetary accounting is feasible in principle but is not identified by the present design. A consumer-expenditure measure would combine a causal national counterfactual price wedge with product-specific quantities sold over the event window, $C_e^{\text{retail}} = \sum_{t \in e} Q_t(p_t - p_t^0)$. This object measures additional expenditure, not social welfare loss, because part of the price payment is a transfer within the supply chain. Real resource costs would additionally require vessel-level lost payload, route-specific freight rates, rerouting costs, inventory drawdowns, and production losses. The AIS data observe crossings and reported draught but not cargo tonnage, vessel capacity, freight contracts, or inventories. The current estimates can therefore support transparent scenario bounds once official monthly product deliveries are added, but not a defensible point estimate of total economic damage.

3. Transport Disruption and Retail-Price Responses

The results answer four questions in sequence. First, do persistent navigation constraints reduce realized tanker movement? Second, do German national price changes depart from comparable EU price changes during low-water stress? Third, do prices move differently within Germany in markets with greater baseline AIS tanker dependence? Fourth, do event-time, availability, and substitution diagnostics support a scarcity interpretation? Table 4 previews the answer: the tanker-movement association is coherent but inference-sensitive; national price differences are positive but have coarse country-placebo ranks; and regional gradients are statistically unresolved.

The main evidence chain contains four empirical objects: the AIS tanker-crossing response, national EOB price differences, regional AIS-dependence gradients, and dynamic guardrails. Discrete threshold-source splits, sample-window checks, reconstructed availability outcomes, control variants, infrastructure interactions, high-water results, and aggregate rail context are secondary diagnostics and are reported in the appendix. They qualify the interpretation but do not define additional headline findings.

The regional price coefficients are reduced-form local retail-price gradients, not structural transport-cost elasticities or average national price changes. The EOB coefficients instead describe weekly national German price changes relative to fixed EU donor weights. The regional coefficients show whether more AIS-dependent grid cells have different fuel prices than less dependent grid cells on the same date when a navigation event occurs.

Sections 3–4 follow that evidence chain: AIS crossings establish the transport response; Table 6 and Figure 3 report national price differences; Table 7 and Figure 4 report regional gradients; event-time diagnostics test onset dynamics; and Section 4 evaluates observable adjustment margins.

3.1. Overview

Table 4 distinguishes the paper's central result from its qualifications. The transport result is a coherent but inference-sensitive AIS response: mixed/fallback low-water stress is associated with 4.7 percent fewer crossings ($p = 0.084$), a 2.3-percentage-point lower crossing probability, and lower crossing speed under waterway-and-date clustering. National diesel breadth and depth estimates are positive relative to fixed European controls, but country-placebo ranks remain coarse and Germany-specific confounding is unresolved. In the internally frozen regional model, the primary diesel low-water constraint is positive and marginal at the ten-percent level; gasoline threshold estimates are imprecise, and no secondary depth or high-water coefficient survives Holm adjustment. The event study has a strongly rejected joint pretrend test.

3.2. AIS Tanker Disruption

AIS positions alone cannot distinguish movement from waiting because a stationary tanker continues to transmit. We therefore link consecutive positions into movement segments and count a crossing only when a segment intersects a gauge-centered cross-section. The resulting gate-day count measures realized passage through a river corridor rather than the number of transmitted positions.

The crossing lines are constructed around PEGEL gauges. For each gauge, the local waterway direction is inferred from neighboring gauges on the same official waterway, and a short cross-section is drawn perpendicular to that direction. AIS pings are sorted by vessel identifier and timestamp, implausibly long time gaps or spatial jumps are dropped, and remaining movement segments are intersected with these cross-sections. The resulting panel is observed at the gauge-day-direction level and records crossing counts, unique vessels, average speed at crossing, and average draught at crossing. More specifically, the analysis focuses on ships of type codes 81–84, to investigate the potential impact of disruptions on product, chemical, and related tanker traffic.

The corresponding first-stage specification is

$$\log(1 + \text{Ship}_{ft}) = \alpha_f + \lambda_t + \beta_1 \text{Low}_{ft} + \beta_2 \text{High}_{ft} + \beta_3 \text{NSB}_{ft} + u_{ft}, \tag{7}$$

where Ship_{ft} denotes tanker activity at crossing location f on date t, measured by crossing counts, an indicator equal to one if at least one tanker crosses the gate that day, average speed at crossing, or average draught at crossing; α_f are crossing-location fixed effects; and λ_t are date fixed effects.

Average observed draught is the mean AIS-reported vertical distance between the waterline and keel among vessels crossing a gate on that day. Because AIS draught fields may be stale or missing, this outcome is interpreted as a descriptive load proxy rather than a precise cargo measure.

Table 4: Overview of findings

This table summarizes the main findings. AIS crossing estimates are the primary transport-disruption evidence. The national EOB entries are weekly percentage-point changes relative to fixed EU donor weights; breadth and depth enter separate models. Regional retail-price entries are same-date gradients or event-time diagnostics. None is a structural transport-cost pass-through estimate. The internally frozen regional rows use federal-state-by-date fixed effects and report the low-water threshold and additional depth gradients separately. The calendar-and-regional row distinguishes explicit named-calendar controls, which leave the less restrictive estimates nearly unchanged, from the stricter within-state-and-date comparison. Panel C synthesizes several adjustment diagnostics and therefore has no single common coefficient.

Evidence block	**Outcome or comparison**	**Estimate / status**	**(SE)**	**Interpretation**
Panel A. Primary transport evidence				
AIS tanker crossings	Low-water tanker crossings	-4.7^{*}	(2.6)	Primary evidence of realized tanker-logistics disruption.
Panel B. National price changes and regional exposure gradients				
National weekly net-price difference	Diesel: breadth / depth	$+0.271/+0.154$	(0.097/0.050)	Breadth (+10 pp) / depth (+1 cm), in pp; HAC-positive but weak country-placebo ranks.
	Euro 95: breadth / depth	$+0.196/+0.145$	(0.100/0.051)	
Frozen regional gradient: low-water constraint	Diesel	$+0.25^{*}$	(0.14)	Small, mixed, and unresolved under state-by-date fixed effects and two-way clustering.
	E5	−0.11	(0.17)	
	E10	−0.07	(0.17)	
Calendar and regional checks	Explicit calendars / state-by-date FE	Unchanged / attenuated		Named calendar controls leave gradients unchanged; state-by-date FE attenuate them.
Frozen regional gradient: additional depth	Diesel	−1.18	(0.64)	Mixed and unresolved after Holm adjustment; no monotone scarcity gradient.
	E5	+0.98	(0.67)	
	E10	+0.76	(0.70)	
Regional dynamic gradient	Event-study post mean	+0.036	–	4 post coefficients are pointwise positive, but the joint pretrend test rejects (p=7.1e-10).
	Matched diesel contrast	-0.794^{**}	(0.336)	19 exact-state matched events; the similarly negative pre-event coefficients indicate a persistent level difference rather than an onset break.
Panel C. Adjustment margins, buffers, and context				
Adjustment and buffer diagnostics	BASt, pipeline, public supply, and rail	Qualitative synthesis		No observed margin establishes systematic buffering or local rerouting; positive pipeline and public-supply interactions run against a simple buffer interpretation, and rail data are aggregate context.

Table 5 reports gauge-crossing regressions of tanker movement on the preferred low-water navigation-constraint, and, for completeness, also for the high-water navigation-restriction, and high-water closure-state indicators. The indicators are set to one only for episodes lasting at least five consecutive days. In the mixed-threshold series, low-water stress is associated with 4.7 percent fewer crossings ($p = 0.084$) and a 2.3-percentage-point lower probability of any crossing ($p = 0.094$). Average crossing speed falls by 0.229 units and is precisely estimated. The high-water restriction count estimate is similarly marginal, while the complete closure-state count contrast is negative but imprecise. The transport evidence is coherent across movement outcomes but sensitive to waterway-level inference. The balanced gate-day split assigns the negative low-water association to fallback episodes; the official coefficient is uninformative because its support consists of two nearly inactive Danube gates. For details, see Appendix Table F.3. Figure 2 provides a descriptive event-time diagnostic for distinct transitions. A delayed decline is visible across all three panels: low-water crossing incidence is significantly lower on days 8 and 9, the high-water-restriction panel falls significantly on days 6 and 7, and the closure-transition panel reaches a significant decline on day 5. This approximately one-week timing is consistent with delayed loading, dispatch, or route-adjustment responses rather than an instantaneous shutdown at the hydrological threshold. It remains suggestive rather than a separate causal estimate because the intervals are pointwise, the high-water samples shrink after subsequent threshold transitions, and several pre-event coefficients are also volatile.

The physical depth mechanism does not begin at a discrete additional 30 cm buffer: without a buffer, another 10 cm of deficit is associated with 4.2 percent fewer tanker crossings, while hinges at 10–40 cm remain negative but fit progressively worse. This is consistent with the GDWS fairway-depth formula: the 30 cm Flottwasser is an under-keel safety allowance, while available fairway depth itself changes continuously with the gauge deviation from GlW (Generaldirektion Wasserstraßen und Schifffahrt, 2023). For details, see Appendix Table A.12.

Table 5: Navigation constraints reduce tanker crossings

This table reports gauge-day first-stage estimates relating persistent navigation events to realized tanker crossings in the AIS panel restricted to AIS ship type codes 81–84. Crossings are counted when a vessel movement segment intersects a gauge-centered cross-section line. The dependent variables are the logarithm of one plus tanker crossings, an indicator for any tanker crossing at the gauge on the day, average speed at crossing, and average observed draught at crossing. Low-water navigation constraints, high-water navigation restrictions, and high-water closure conditions are measured at the corresponding PEGEL gauge and retained only when the episode lasts at least five consecutive days. The high-water closure-state row is the linear combination of the restriction and incremental HSW coefficients. The headline indicators combine official and fallback threshold definitions; the split shows that fallback episodes identify the negative low-water association. For details, see Appendix Table F.3. All specifications include crossing-gate and date fixed effects. Standard errors are two-way clustered by waterway and date; gate-and-date clustering is reported as an inference sensitivity.

	$\log(1 + \text{Crossings})$	Any crossing	Average speed	Average draught
Low-water constraint (mixed thresholds)	-0.048* (0.027)	-0.023* (0.013)	-0.229*** (0.067)	-0.007 (0.033)
High-water navigation restriction	-0.038* (0.019)	-0.030* (0.017)	-0.830*** (0.123)	-0.246 (0.176)
High-water closure state	-0.051 (0.038)	-0.058 (0.046)	-0.451 (0.372)	0.075 (0.248)
Gate FE	Yes	Yes	Yes	Yes
Date FE	Yes	Yes	Yes	Yes
Waterway and date clustered SE	Yes	Yes	Yes	Yes
Mean dep. var.	0.275	0.231	8.448	4.248
Observations	124152	124152	28648	28648
Within R^2	0.001	0.001	0.002	0.000

Figure 2: Tanker-crossing incidence around distinct navigation-stress transitions

The figure plots changes in the probability of any tanker crossing, in percentage points, around distinct mixed-threshold navigation transitions. Crossings are measured at gauge-centered AIS cross-sections for AIS ship type codes 81–84. Low-water starts require no navigation-event exposure at the same gate during days -14 to -1. High-water restriction starts exclude simultaneous closure-threshold exceedance and are censored when that threshold is subsequently crossed. The closure-transition panel allows a preceding restriction and is normalized to restricted day -1. Pointwise significant declines appear approximately one week after transition: days 8–9 for low water, days 6–7 for high-water restriction, and day 5 for the HSW transition. These are descriptive timing patterns, not simultaneous-confidence-band results. Facet headers report event counts; shaded bands are pointwise 95 percent confidence intervals with standard errors clustered by crossing gate.

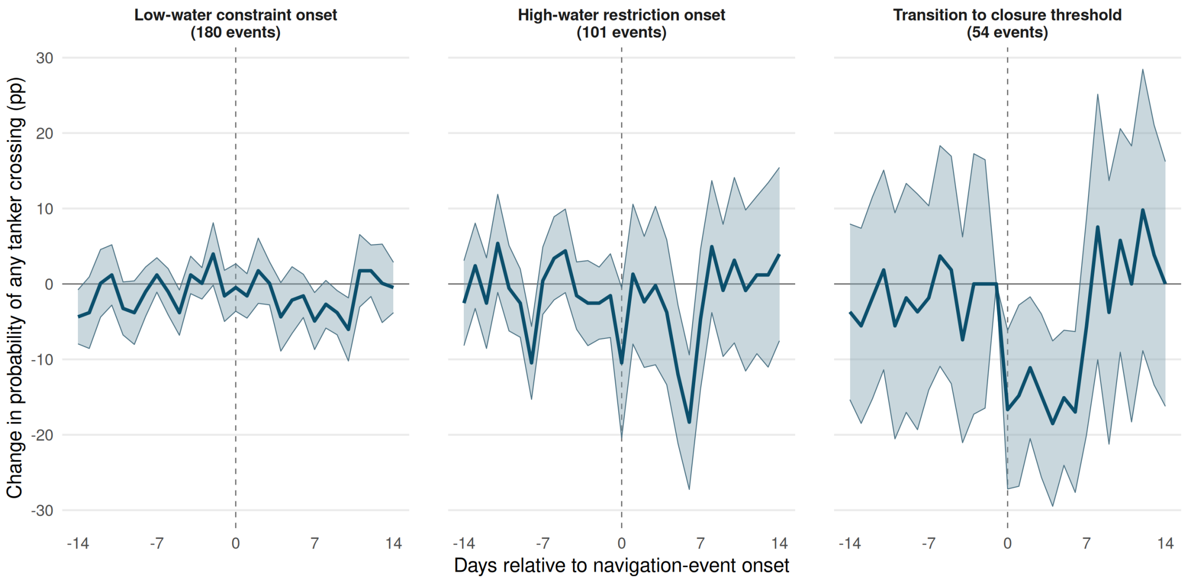

3.3. National Price Differences

Table 6 reports the national weekly specification in Equation (2). A 10-percentage-point increase in the equally weighted share of major corridors under persistent low-water stress is associated with a 0.271-percentage-point larger German weekly net diesel-price change and a 0.196-point larger Euro 95 change relative to their synthetic EU controls. One additional centimeter below the operative threshold is associated with net-price differences of 0.154 points for diesel and 0.145 points for Euro 95. Tax-inclusive estimates remain positive and somewhat smaller.

Table 6: Weekly German price changes relative to synthetic EU controls

The outcome is 100 times the weekly log-price change in Germany minus the same fixed-weight change among donor countries in the European Commission's Weekly Oil Bulletin. Nonnegative donor weights sum to one and are fitted to net-of-tax weekly changes during 2009–2013; the same weights are used for tax-inclusive prices. Hydrology uses equal fixed weights for the Rhine, Elbe, Weser, and Danube; breadth and depth enter separate regressions with year and calendar-month fixed effects. Parentheses contain Bartlett HAC standard errors with eight weekly lags, and stars use Holm-adjusted p-values within each fuel-price family. The net-price country-placebo ranks are 0.067 for both diesel estimates and 0.133 for both Euro 95 estimates. Each regression has 609 weeks through June 2026. The estimates are national associations, not causal synthetic-control effects.

Outcome	**Hydrological variable**	**Diesel**	**Euro 95**
Net of tax	Low-water share (+10 pp)	0.271*** (0.097)	0.196** (0.100)
	Depth below threshold (+1 cm)	0.154*** (0.050)	0.145*** (0.051)
Including tax	Low-water share (+10 pp)	0.205*** (0.079)	0.195* (0.101)
	Depth below threshold (+1 cm)	0.125*** (0.043)	0.134** (0.054)

The conventional HAC intervals do not capture the full design uncertainty. Both diesel estimates attain the minimum possible country rank of 0.067, while the Euro 95 ranks are 0.133. The diesel estimates remain precise with 4, 13, or 26 HAC lags, and six one- to three-year time shifts do not reproduce the positive diesel breadth coefficient. Figure 3 shows that the diesel breadth difference reaches 0.964 percentage points by week four and the depth difference reaches 0.558 points per centimeter; both fade and are imprecise by week eight. The pattern is consistent with temporary national adjustment but does not identify a causal price effect.

Figure 3: Cumulative national net-price differences during low-water stress

The figure reports changes in the German net-of-tax price gap from week $t-1$ through week $t+h$, where the gap is relative to the fixed synthetic EU control in Equation (2). The left panel scales low-water breadth by 10 percentage points; the right panel scales depth by one centimeter. Breadth and depth enter separate models with year and calendar-month fixed effects. Vertical bars are pointwise 95-percent intervals based on Bartlett HAC standard errors with eight weekly lags. Horizon zero is the change from week $t-1$ to the stressed week. Country-placebo ranks are available for the one-week estimates in Table 6, not for every plotted horizon.

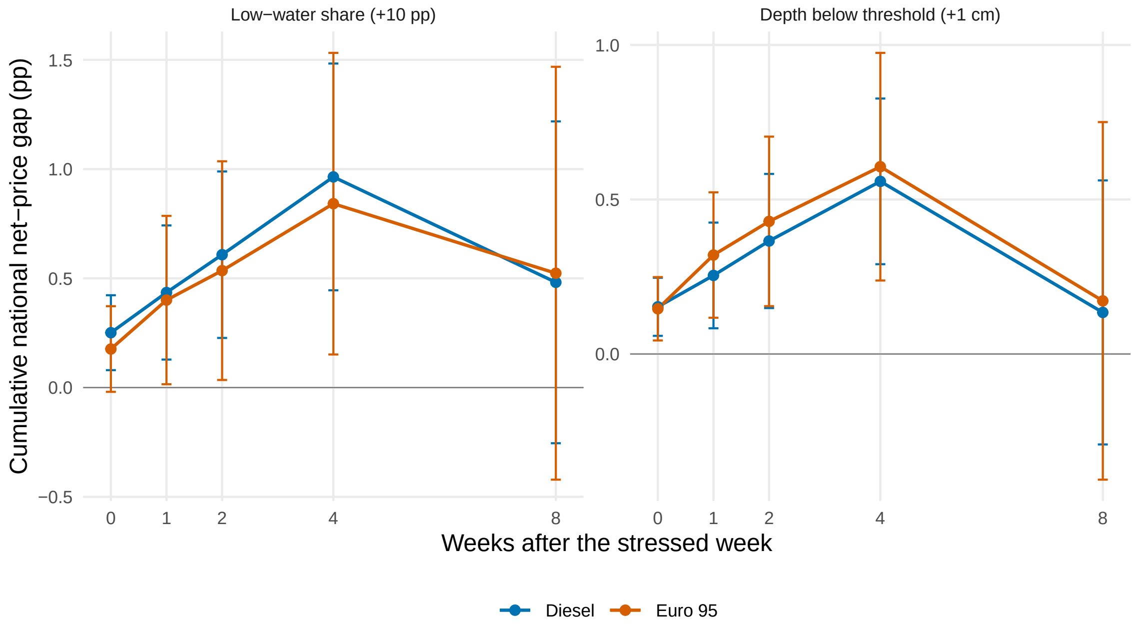

3.4. AIS-Weighted Price Gradients

The preferred price model follows Figure 1. For each river r and grid cell i, baseline AIS tanker dependence A_{ir} is computed before the outcome window and interacted with contemporaneous hydrological conditions on that river. Low- and high-water severity enter symmetrically as meters beyond their operative restriction thresholds, while the HSW indicator allows an additional discontinuity at the official high-water closure threshold:

$$
\begin{aligned}
y_{it} = \theta_L \sum_r L_{rt} A_{ir} + \theta_D \sum_r D_{rt} A_{ir} \\
+ \theta_R \sum_r R_{rt} A_{ir} + \theta_H \sum_r H_{rt} A_{ir} \\
+ \theta_C \sum_r C_{rt} A_{ir} + \mathbf{Z}'_{it}\gamma \\
+ \mu_i + \lambda_{s(i)t} + \varepsilon_{it}.
\end{aligned}
\tag{8}
$$

Here L_{rt} and R_{rt} indicate persistent low- and high-water restrictions; D_{rt} is meters below the operative low-water threshold; H_{rt} is meters above the operative high-water restriction threshold; and C_{rt} indicates crossing the HSW closure threshold. Grid fixed effects absorb the level of predetermined AIS dependence and other stable local attributes. Federal-state-by-date fixed effects absorb shocks shared by grids in the same state on the same day, including the common state-level component of each river-day shock. The coefficients are therefore differential gradients: they ask whether prices move differently across grid cells with greater pre-event dependence on the affected river within the same state and date. DWD weather controls address observed local weather. The preferred model does not condition on tanker deliveries, inventories, availability, or lagged prices because these variables may lie downstream of the hydrological event.

Figure 5 depicts predetermined baseline AIS tanker dependence rather than a fitted price surface. Changing this definition reverses the coefficient: AIS-only mixed-threshold gradients are negative, whereas adding harbor proximity, subtracting pipeline access, or using the weighted composite makes them positive. This does not isolate one omitted confounder; it shows that the indices mix tanker dependence with differently signed supply-geography margins. The weighted composite is therefore a sensitivity analysis, not the main treatment measure. For details, see Appendix Table D.8.

Table 7 reports the preferred no-lag specification. It separates entering each navigation-restriction state from moving farther beyond the corresponding threshold. This distinction avoids interpreting the sign of a threshold indicator as the response to increasingly severe water levels. The coefficients remain reduced-form relative price gradients; Figure 6 and Table 8 assess whether a new differential emerges around onset.

The official-threshold-only diagnostics are not a stable substitute for the internally frozen mixed-threshold model. In the state-day standalone specification, the official gradients are +0.014, +0.047, and +0.045 percent for diesel, E5, and E10. In the date-fixed-effects source split, the corresponding official coefficients are +0.005, +0.095, and +0.093 percent. Alternative regional controls shift these estimates again. The threshold-source tables are therefore reported as support and specification diagnostics rather than as a second headline result. For details, see Appendix Tables A.1 and A.7.

Conditional significance in one threshold-source specification does not establish a causal scarcity response. The relevant question is whether the sign and magnitude persist across the internally frozen state-day model, depth parameterizations, and dynamic diagnostics; they do not.

The timing battery shifts mixed-threshold events 30 and 45 days earlier, 30 days later, 52 weeks earlier, 52 weeks later, and 104 weeks earlier. Every model retains the four companion hydrological gradients, DWD weather controls, grid fixed effects, and federal-state-by-date fixed effects. The battery also includes a wrong-river assignment, a below-median-exposure subsample, and 100 fixed-seed within-region exposure permutations. The 45-day gasoline leads, wrong-river gasoline assignments, and low-exposure estimates are nonzero even though the permutation distribution is centered near zero. These failures qualify river-specific causal isolation rather than supplying another set of headline estimates. For details, see Appendix Tables A.6 and D.9.

The aligned leave-one-river-out estimates reinforce this caution. The diesel coefficient is +0.251 percent in the full model, +0.080 percent when the Rhine contribution is removed, and +0.375 percent when the Elbe contribution is removed; precision changes accordingly. The sign remains positive, but magnitude and inference rely materially on those two river histories. For details, see Appendix Table D.10.

Table 7: Static price gradients by baseline AIS tanker dependence

This table reports the internally frozen post-baseline differential price gradients from July 1, 2021, through June 30, 2026. Low-water depth is measured in meters below the operative threshold; high-water excess is measured in meters above the restriction threshold; and the HSW row is the additional closure-threshold shift. All models include grid and federal-state-by-date fixed effects and DWD weather controls, omit lagged prices and downstream adjustment variables, and two-way cluster standard errors by grid and date. The diesel low-water constraint is the primary coefficient. Stars on secondary outcomes use Holm-adjusted p-values within fuel. The internal registry was frozen on July 19, 2026, after exploratory analysis; it is not a preregistration.

AIS-dependence shock	**Diesel**	**E5**	**E10**
Panel A. Low-water conditions			
Persistent constraint × AIS dependence	0.251*	-0.109	-0.067
	(0.141)	(0.168)	(0.174)
Additional depth deficit × AIS dependence	-1.183	0.977	0.758
	(0.640)	(0.670)	(0.697)
Panel B. High-water conditions			
Navigation restriction × AIS dependence	-0.141	0.269	0.329
	(0.237)	(0.162)	(0.165)
Additional water-level excess × AIS dependence	0.179	-0.773	-0.910
	(0.477)	(0.394)	(0.413)
Additional HSW-threshold shift × AIS dependence	0.331	1.092	1.195
	(0.621)	(0.634)	(0.644)

In the less restrictive grid-and-national-date benchmark, subtracting the German daily mean reproduces the coefficients exactly. The preferred state-by-date model instead compares grids within the same federal state and date. Its low-water constraint gradients are +0.251 percent for diesel, −0.109 percent for E5, and −0.067 percent for E10. The diesel estimate is marginal at the ten-percent level and the gasoline estimates are imprecise. The regional evidence therefore supports neither a robust widening nor a robust narrowing of the tanker-dependence price gap.

Figure 4: Flexible regional price gradients across low-water depth bins

For each river-day, average depth below the operative threshold is divided by the share of gauges in persistent low-water restriction to recover mean depth among affected gauges. The four bins enter jointly, interacted with standardized baseline AIS tanker dependence; the remaining high-water terms, DWD weather controls, grid fixed effects, and federal-state-by-date fixed effects are unchanged. Coefficients are relative price gradients for a one-standard-deviation increase in dependence on the affected river. Vertical bars are pointwise 95-percent intervals based on grid-and-date clustered standard errors. Percentages below the bin labels report the gauge-day-weighted support among persistent low-water observations.

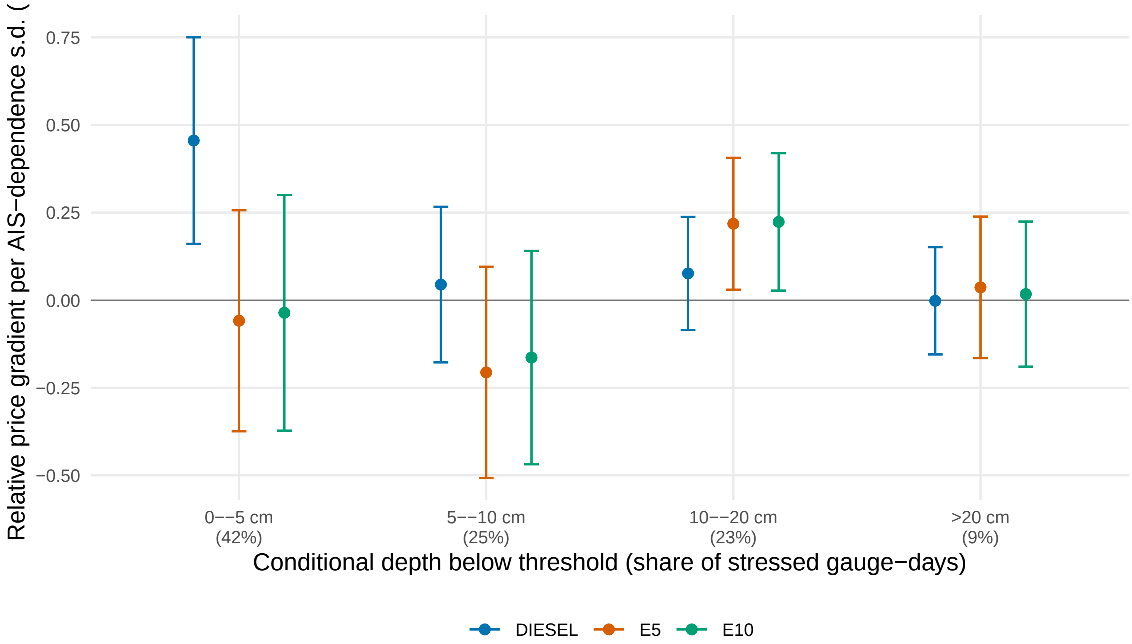

Figure 4 rejects a monotone depth profile. The 0–5 cm bin is positive and precise only for diesel; the 5–10 cm estimates are small for diesel and negative for gasoline; the 10–20 cm gasoline estimates turn positive; and all three estimates above 20 cm return toward zero. A continuous-at-threshold raw-depth model yields small positive but imprecise slopes for all three fuels, whereas gauge-standardized deficits yield small negative gradients. Buffer hinges become positive for gasoline only at the largest explored knots, where support is sparse and the exercise spans multiple candidate thresholds. No parameterization therefore recovers a stable monotone scarcity gradient. For details, see Appendix Table A.11.

Table 7 does not reveal a monotone scarcity response. In the preferred state-day model, the diesel threshold gradient is positive and marginal, while the gasoline threshold gradients are negative and imprecise. The additional depth gradient is negative for diesel and positive for E5 and E10, but none survives Holm adjustment. High-water restriction, excess, and HSW terms are likewise mixed and unresolved. Explicit federal-state public-holiday, adjacent-day, and school-vacation controls leave the less restrictive grid-and-date estimates nearly unchanged. Federal-state-by-date fixed effects alter the comparison more materially by absorbing the full set of state-specific daily demand and supply shocks. The sensitivity is therefore not attributable to the observed calendar alone. For details, see Appendix Tables A.9 and A.8.

Differential pass-through of the 2022 German fuel-tax cut does not explain the mixed low-water pattern.

The Tankrabatt interaction is -0.017 percent for diesel, -0.083 percent for E5, and -0.069 percent for E10, and is statistically insignificant in every case. Adding it changes the threshold gradients by at most 0.09 percentage points and the depth gradients by at most 0.23 percentage points; the signs of the corresponding low-water terms are unchanged. For details, see Appendix Table A.10.

At observed mean prices, the internally frozen low-water threshold gradients correspond to approximately $+0.43$ euro cents per liter for diesel, -0.20 cents for E5, and -0.12 cents for E10 per one-standard-deviation increase in baseline tanker dependence. The diesel event-study post mean is about $+0.06$ cents per liter. The matched contrast is larger at -1.35 cents, but the same gap is already visible before onset and is not interpreted as an event effect. For details, see Appendix Table A.2.

Nonpositive price messages may encode genuine product scarcity, but they may also record station closure, maintenance, or reporting-state changes. Reconstructed nonavailability is therefore treated as a separate extensive-margin outcome rather than an extreme price. Under the full mixed-threshold specification, no station-count-weighted primary margin survives Holm adjustment. The E10 product-specific estimate is negative and conventionally significant before adjustment (-0.412 percentage points; unadjusted $p = 0.039$, Holm $p = 0.154$), while the all-fuels estimate is -0.104 points ($p = 0.316$). For details, see Appendix Table A.3. The secondary stress outcomes do not reveal a robust differential response either. The spatial-IQR effects are -0.445, -0.111, and -0.186 cents per liter for diesel, E5, and E10, respectively. Time-weighted intraday standard deviations increase by 0.061, 0.132, and 0.141 cents per liter. Event-based realized variation increases by 0.092, 0.380, and 0.500 cents per liter. The E5 and E10 standard-deviation estimates and the E10 event-variation estimate have unadjusted p-values below 0.10, but none of the nine estimates survives the joint Holm correction. These outcomes therefore provide no multiplicity-robust evidence that low-water stress disproportionately increases either spatial price dispersion or intraday repricing in more tanker-dependent grids. For details, see Appendix Table A.4.

The mixed-threshold gradient can be compared in the internally frozen July 2021–June 2026 sample and the shorter July 2021–November 2022 AIS-overlap window, separating sample-window sensitivity from threshold-source and regional-control sensitivity. For details, see Appendix Table A.5.

The second panel in Figure 5 translates the static mixed-threshold diesel coefficient into a fitted gradient by multiplying it by baseline AIS tanker dependence. Its geography is fixed by pre-event tanker movements, not estimated grid-specific price effects.

Figure 6 reports the event-study diagnostic. It focuses on diesel low-water episodes in corridors with baseline AIS tanker exposure. Events are required to last at least five days and to have a clean 18-day pre-window without low-water, high-water, or non-navigable exposure in the same corridor. The estimating equation is

$$y_{iet} = \sum_{\substack{k=-18 \\ k \neq -7}}^{18} \beta_k \mathbf{1}\{\tau_{et} = k\} D_{ir(e)} + \mathbf{Z}'_{it}\gamma + \alpha_{ie} + \lambda_t + \varepsilon_{iet}, \tag{9}$$

Here y_{iet} is the log diesel price in grid cell i for stacked event e on date t, τ_{et} is event time relative to low-water onset, $D_{ir(e)}$ is baseline AIS tanker dependence on the event river, α_{ie} are grid-by-event fixed effects, and $\lambda_{s(i)t}$ are federal-state-by-date fixed effects. The omitted event day is -7, a clean pre-event day

Figure 5: Baseline AIS tanker dependence and static fitted price gradient

Panel (a) maps the maximum standardized river-specific baseline AIS tanker dependence across grid cells. Dependence is constructed from January–June 2021 tanker crossings and a distance decay from river-specific crossing gates. Panel (b) multiplies this predetermined dependence measure by the mixed-threshold diesel coefficient from Table 7. It is a fitted differential gradient, not a local causal effect. The E5 and E10 maps have the same dependence geography and differ only by the fuel-specific coefficient. Map lines delineate study areas and do not necessarily depict accepted national boundaries.

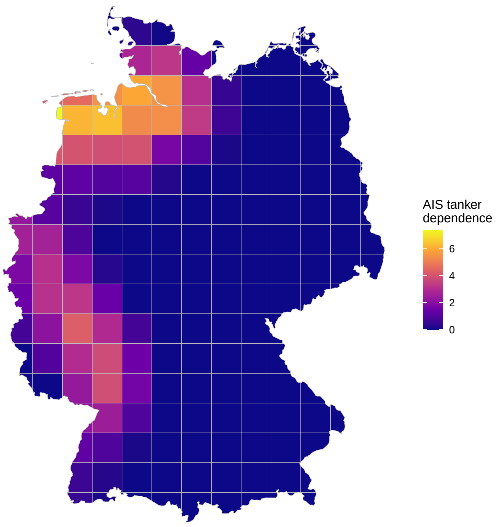

(a) Baseline AIS tanker dependence

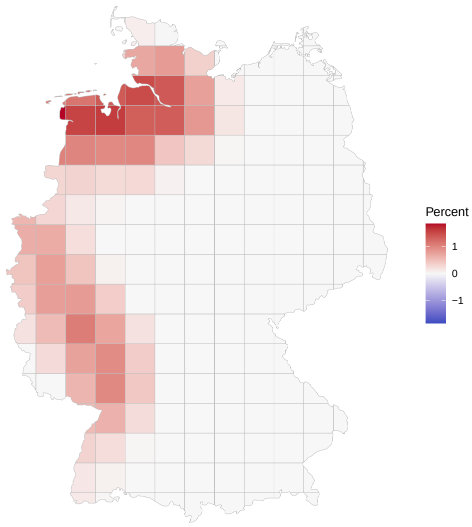

(b) Diesel low-water fitted gradient chosen before the short-run anticipation window immediately before event onset. The treatment gradient is fixed before the event, and standard errors are two-way clustered by grid and event.

The figure reports raw event-time coefficients relative to this omitted pre-event day; it does not subtract the average pre-event coefficient ex post. This keeps the diagnostic transparent: the pre-period directly shows whether more AIS-dependent grid cells were already moving differently before the low-water episode, while the post-period shows whether there is an additional break around event onset.

Figure 6: Diesel low-water event study with federal-state-by-date fixed effects

The figure plots event-time coefficients from stacked diesel-price regressions that interact low-water episode timing with river-specific baseline AIS tanker dependence. Event time is measured relative to the start of a low-water episode lasting at least five days. The sample uses all AIS-covered corridors and keeps events with no hydrological episode in the same corridor during the 18-day pre-window. The omitted period is day −7. The specification includes grid-by-event and federal-state-by-date fixed effects and DWD weather controls, omits lagged prices, and two-way clusters standard errors by grid and event.

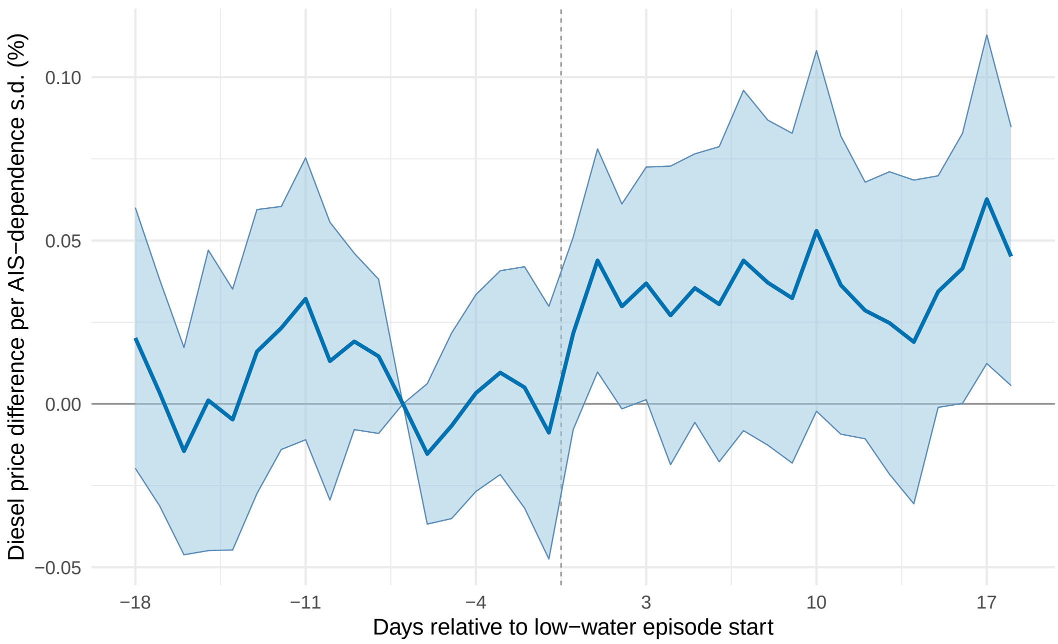

After requiring every candidate event to have all 18 pre-event dates observed, the event study retains 41 episodes. The mean post-onset gradient is +0.036 percent, and 4 of 19 post coefficients are individually positive at the five-percent level. No individual pre-event coefficient is significant, but the joint test strongly rejects zero pre-event coefficients ($p = 7.1 \times 10^{-10}$). The post-onset pattern therefore cannot be interpreted as a clean causal break at the low-water threshold; it remains consistent with anticipatory, gradual, or residual differential adjustment.

3.5. Matched Stacked-Event Robustness

As a final identification check, the analysis constructs a matched stacked-event sample around official five-day low-water episode starts. Treated grids are above the 75th percentile of event-river baseline AIS tanker dependence, while donor grids are at or below the median in the same federal state. Up to three donors are matched to each treated grid on pre-event diesel prices, pre-event trends, DWD weather, station density, pipeline access, inland-harbor proximity, and distance to the nearest OSM-derived petroleum supply node. The estimating sample keeps the $[-18, +18]$ event window and absorbs treated-grid-by-event-pair fixed effects and federal-state-by-date fixed effects. The reference day in the event-study version remains day -7.

Table 8: Matched stacked-event diesel estimates

The table reports treated-control diesel-price contrasts for 19 matched official low-water events. Treated grids are above the event-river 75th percentile of baseline AIS tanker dependence; controls are at or below the median in the same federal state and are matched on pre-event price dynamics, weather, station density, pipeline access, inland-harbor proximity, and OSM-derived petroleum supply-node distance. A rotated wrong-river matched design is not reported because the AIS-only treatment definition leaves no common support. The static wrong-river placebo remains nonzero. For details, see Appendix Table A.6. Specifications include treated-grid-by-event-pair and federal-state-by-date fixed effects. Standard errors are two-way clustered by grid and event. This design is a robustness check, not a separate structural estimand.

Matched design	**Estimate**	**SE**	**Events**	**Grids**
Official low-water matched DiD	-0.794**	0.336	19	88

Figure 7: Matched diesel event study around official low-water starts

The figure plots treated-control event-time coefficients for the 19 matched official low-water events. Event time is measured relative to five-day episode starts. The omitted period is day -7; no pre-event mean subtraction is applied. The specification includes treated-grid-by-event-pair fixed effects, federal-state-by-date fixed effects, and DWD weather controls.

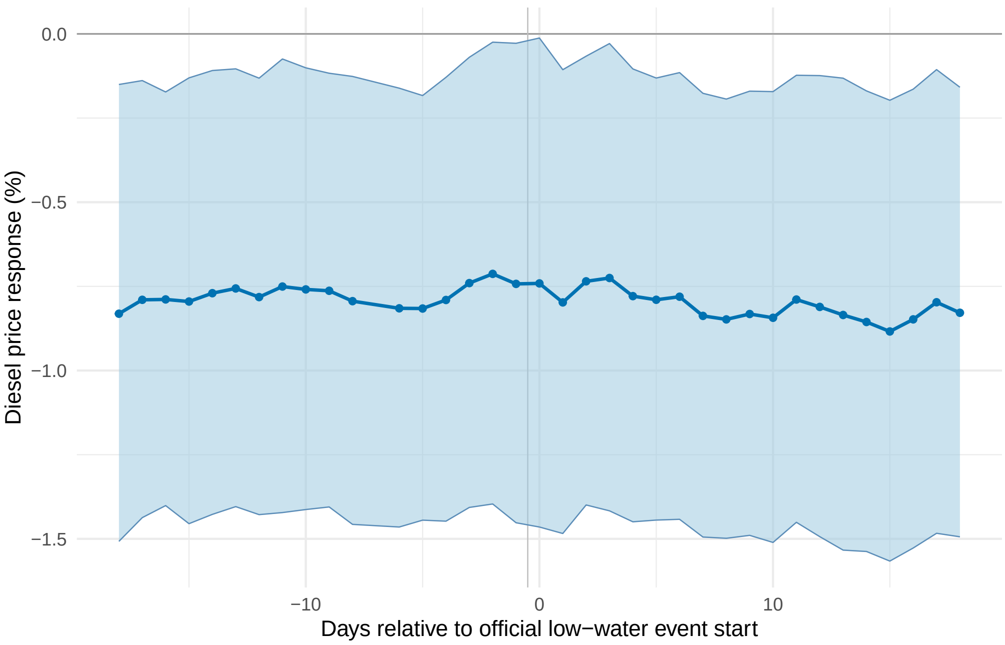

The matched post-period contrast is -0.794 percent with a standard error of 0.336. This is not evidence that low water lowers prices: the event-study coefficients are already about -0.7 to -0.8 percent throughout the pre-period relative to day -7. The design therefore reveals a persistent matched-sample level difference rather than a threshold-onset break. Table C.4 reports matched pre-event balance. Pipeline, harbor, and supply-node variables enter matching separately because they are not components of the AIS treatment measure. Remaining imbalance and the absence of wrong-river common support reinforce the cautious interpretation.

The matched dynamic profile is reported in Figure 7; its pre-event level difference is why the matched contrast is not interpreted as an onset effect.

4. Substitution and Buffering Diagnostics

The previous section established the main hierarchy of evidence: shipping disruption is visible in AIS crossings, while local retail-price responses are heterogeneous and constrained by the dynamic and matched diagnostics. This section studies the remaining adjustment margins. The BASt road-count evidence is used narrowly as a substitution test, and it does not reveal a robust compensating increase in nearby truck or heavy-vehicle traffic. Inland-harbor BASt estimates point instead to weak or lower harbor-related activity. Pipeline heterogeneity provides only limited evidence that potential grid-level pipeline access explains or attenuates retail-price gradients. These exercises therefore discipline the resilience interpretation rather than completing a full shipment-flow accounting.

4.1. Road Substitution

The second mechanism question is whether road traffic changes when inland-waterway transport becomes more difficult. The BASt panel measures all trucks and heavy vehicles, not fuel tankers specifically. The sign is therefore not unambiguous ex ante. A positive response near affected gauges would be consistent with aggregate substitution toward road haulage, but it could reflect non-fuel freight. A negative response around inland harbors would be consistent with fewer vessel arrivals generating less local collection and delivery traffic. The BASt exercise can detect these broad margins but cannot isolate road-based fuel transport.

The corresponding station-day specification is

$$\log(1 + \text{Road}_{it}) = \alpha_i + \lambda_t + \theta \text{Affected}_{it} + v_{it}, \tag{10}$$

where Road_{it} denotes night-time truck or heavy-vehicle traffic at BASt station i on date t, α_i are station fixed effects, and λ_t are date fixed effects. Night-time traffic is measured over BASt hours 23, 24, and 1–6, corresponding to the 22:00–06:00 window. A BASt station is defined as affected on a given date if it is in the same river basin as a PEGEL gauge experiencing a hydrological episode, lies within 50 kilometers of that gauge, and the hydrological episode lasts at least five consecutive days. The analysis is restricted to BASt stations located in AIS-relevant river-basin corridors. This definition is finer than the coarse corridor aggregation because exposure varies at the station-day level and is tied to nearby stressed gauges rather than to the average hydrological state of an entire basin.

The affected-station design does not show a compensating road-freight increase. Low-water exposure is associated with 1.3 log points lower night-time truck counts and 1.2 log points lower night-time heavy-vehicle counts, neither precisely estimated. High-water exposure is close to zero for night-time truck counts and negative but imprecise for heavy-vehicle counts. The complete closure-state contrast is also negative and imprecise for night-count outcomes, although the night-time heavy-vehicle share falls significantly. For details, see Appendix Table G.1.

This result is useful for interpretation. The AIS crossing evidence shows a clearer disruption margin for tanker movements, but even a finer BASt exposure definition does not reveal a robust increase in aggregate road freight near affected gauges. This could mean that substitution occurs through routes not captured by the 50-kilometer gauge buffer, through rail or pipeline capacity, through inventory adjustment, or through changes in load factors rather than visible increases in truck counts. Public monthly rail-freight data also cannot identify local rerouting because they are available only at the national product level. For details, see Appendix Table H.1. The BASt results therefore discipline the mechanism story: road substitution remains plausible, but it is not directly identified in the current BASt station-day specification.

As an additional diagnostic, the analysis also estimates an inland-harbor-catchment version of the BASt exercise. This specification is motivated by a different prediction. If inland navigation is disrupted, truck activity near inland harbors could fall because fewer vessels arrive and depart. Coastal gateways are not used in the main analysis because any re-routing through seaports may be absorbed by pipelines, rail, storage, or road routes outside the local BASt catchments. The analysis therefore assigns BASt stations within 10 kilometers of a documented major German inland harbor or terminal to its catchment; the retained locations are inland rather than coastal gateways. For details, see Appendix Table G.2. Exposure is activated when the harbor's river basin experiences a hydrological episode lasting at least five consecutive days. This distinction makes the exercise a harbor-specific mechanism check rather than a general affected-gauge specification.

The harbor analysis supports the same interpretation as the affected-station exercise: observable truck traffic does not robustly increase around the most plausible inland-harbor catchments. Night-time truck and heavy-vehicle counts are slightly lower during low-water episodes, with estimated effects of -0.9 and -1.4 log points; high-water and closure-risk count estimates are positive but imprecise. For details, see Appendix Table G.3.

Broadening the traffic window does not uncover a road-traffic increase around inland harbors: full-day low-water estimates are -1.3 log points for trucks and -2.2 log points for heavy vehicles, with the latter statistically significant. For details, see Appendix Table G.4. The weekday-adjusted event-study profiles likewise show no compensating road-traffic surge. For details, see Appendix Figure G.4. The strongest evidence for reduced inland-harbor activity therefore comes from the station-day regressions.

The coefficient plots convey the same absence of a robust road-freight increase. For details, see Appendix Figures G.2 and G.3.

4.2. Infrastructure-Based Resilience

The third mechanism question is whether retail-price gradients during river shocks depend on alternative infrastructure. Pipeline geodata provide one such resilience margin, but the relevant empirical object is not simply whether a pipeline crosses a grid cell. A pipeline can buffer local fuel markets only if product can plausibly enter or exit the network nearby. The analysis therefore distinguishes line proximity from potential pipeline access, using nearby network dead ends and junctions in oil-like pipeline geometries as a coarse proxy for locations where the pipeline network may connect to terminals, refineries, storage, or distribution infrastructure.

The corresponding heterogeneity specification augments the baseline model as follows:

$$y_{it} = \alpha + \mathbf{X}_{tf}'\beta + (\mathbf{X}_{tf} \times \text{PipeAccess}_i)'\,\phi + \mu_i + \lambda_t + \rho y_{i,t-50} + \varepsilon_{it}, \tag{11}$$

where PipeAccess_i denotes potential pipeline access within 50 kilometers of grid cell i. The interaction coefficients ϕ measure whether alternative infrastructure dampens or amplifies the transmission of river shocks to local fuel prices.

The pipeline layer is constructed from OpenStreetMap-derived German pipeline geometries. The code retains oil-like pipeline features, maps them to the same 50-kilometer fuel-price grid used in the baseline analysis, and computes line-based measures such as pipeline length, pipeline presence, and distance to the nearest pipeline. It then extracts potential access nodes from the oil-like pipeline network by snapping line endpoints in the projected coordinate system and retaining network dead ends and junctions. The main heterogeneity exercise uses an indicator for whether a grid cell lies within 50 kilometers of one of these potential access nodes. This is more defensible than simple line proximity, but it remains a coarse proxy: it does not observe product type, physical offtake equipment, flow direction, terminal capacity, storage, or contractual access.

The grid-and-date-fixed-effects pipeline test does not support a simple buffering interpretation: the diesel low-water difference is positive, meaning that the AIS-dependence gradient is larger, not smaller, in grids with potential pipeline access on the same date. For details, see Appendix Table E.1. This diagnostic retains the lagged-price control and is not part of the preferred no-lag price model.

The older month-fixed-effects contrasts describe heterogeneous signs by pipeline access but do not supersede the date-fixed-effects comparison used for the main price design. For details, see Appendix Table E.2 and Appendix Figure E.1.

Because pipeline access may also proxy for industrial location, an inland-harbor triple interaction tests attenuation specifically in places with stronger waterway dependence, net of the broader access-versus-no-access difference outside inland-harbor catchments. The refreshed estimates are imprecise across fuels and hydrological regimes; none is statistically distinguishable from zero at the 5-percent level. They therefore do not establish a systematic pipeline-buffering channel. For details, see Appendix Table E.3.

The pipeline results therefore provide only limited evidence that potential pipeline access systematically buffers retail fuel prices against hydrological stress in the current specification. This does not imply that pipelines are irrelevant for fuel logistics. Rather, even the improved access proxy cannot observe effective offtake rights, terminal operations, inventory behavior, or the direction of product flows. The result is still informative for interpretation: unlike the coherent but inference-sensitive AIS disruption evidence, pipeline access does not by itself explain much of the observed heterogeneity in retail-price responses.

The public supply data sharpen this conclusion without converting it into a causal buffering test. From 2014 onward, road-diesel imports are 5.59 percent above their same-calendar-month benchmark in widespread official low-water months, but the estimate falls to 0.63 percent after adding year fixed effects ($p = 0.886$).

The import series therefore does not support a robust aggregate sourcing response, much less one attributable to EU partners; it reports neither bilateral origins nor entry routes. Petroleum handling nevertheless falls at several major inland ports. The UTV capacity interaction is positive for E5 and E10 and near zero for diesel, but terminal capacity is endogenously located near refineries, ports, and dense markets and cannot be read as a storage treatment effect. For details, see Appendix Tables E.6–E.8 and Figures E.3–E.4.

4.3. Synthesis and Interpretation

Table A.16 organizes the evidence into low-water states, high-water states, and the pipeline-access diagnostic. Within each state, it separates transport outcomes from static retail-price gradients. Panel A shows the central asymmetry. Mixed/fallback low-water stress is associated with fewer tanker crossings. The primary diesel regional threshold gradient is positive but only marginal at ten percent; gasoline threshold estimates are imprecise, and secondary depth coefficients do not survive Holm adjustment. Flexible depth specifications are nonmonotone, and the event-study, matched, and nonavailability diagnostics do not identify a clean positive onset effect. Panel B shows negative tanker-movement associations for high-water restrictions and HSW states. In the price model, restriction, excess, and incremental HSW coefficients differ in sign across fuels and no secondary coefficient survives multiplicity adjustment. Panel C shows that observed pipeline access does not attenuate the diesel low-water gradient. These differences are not contradictions because AIS measures movement at affected gates, whereas the price regressions compare more- and less-AIS-dependent retail markets on the same date. Inventories, alternative routes, product mix, and terminal access can separate those outcomes. The main message is consequently narrow: navigation stress is associated with less tanker movement, while downstream retail-price responses remain design-dependent and are not summarized by a monotone scarcity gradient.

Named state holidays and school vacations leave the low-water gradients unchanged, whereas federal-state-by-date fixed effects attenuate them. The regional sensitivity therefore concerns broader state-day shocks or the stricter within-state comparison rather than the observed calendar alone.

Taken together, the evidence follows three steps. Low water is associated with less realized tanker traffic. German net-price changes co-move positively with national low-water stress relative to fixed European controls, but coarse country-placebo ranks leave this comparison descriptive. Within Germany, the preferred state-day model does not establish either a widening or a narrowing of the price gap between more- and less-tanker-dependent grids. The national and regional estimates address different comparisons because the regional fixed effects remove common German price movements and identify only differential spatial gradients.

Cross-border market integration remains a plausible but untested mechanism. Aggregate imports do not distinguish partner countries or entry routes, and their stressed-month difference is not robust to year adjustment. The present evidence therefore leaves domestic and cross-border adjustment among the possible explanations; it does not provide positive evidence for a European trade buffer.

A separate July 1–14, 2026 holdout is a useful negative-control case. The official persistent-low-water share was already 43 percent on June 30, remained below one-half through July 7, and then exceeded 90 percent on July 9. The large national price jump around the turn of the month therefore precedes the sharp broadening of measured stress. The high-minus-zero AIS-dependence gap remains near zero for diesel and is negative for gasoline. This timing and the concurrent national and international shocks prevent attribution of the national increase to low water. For details, see Appendix Table E.9 and Figure E.5.

5. Conclusion

The conclusions distinguish three estimands. Low water is associated with less realized tanker traffic. German net-price changes co-move positively with low-water stress relative to fixed European controls, but the national evidence remains descriptive. The preferred regional model does not establish a larger or smaller local response in more tanker-dependent markets. The national and regional estimates can coexist because the regional fixed effects absorb common German price movements. The conclusions distinguish three estimands. Low water is associated with less realized tanker traffic. German net fuel prices temporarily rise relative to fixed European controls, but the national evidence remains suggestive. The preferred regional model does not establish a larger or smaller local response in more tanker-dependent markets. The national and regional patterns are compatible because the regional fixed effects absorb common German price movements. The evidence therefore contains a positive national relative-price association that is not mirrored by a robust differential gradient in tanker-dependent regions; neither comparison identifies a causal hydrological price effect. This paper shows why transport disruption and downstream retail-price responses must be evaluated separately. Combining high-frequency Tankerkönig fuel prices, PEGELONLINE water-level data, DWD weather controls, AIS vessel movements, BASt road counts, and pipeline geodata, the analysis traces both realized transport disruption and retail-price gradients. The clearest result is the coherent association between persistent navigation stress and reduced realized tanker movement. The low-water count estimate is identified by mixed and fallback-threshold episodes in 2021–2022 and is marginal under waterway-and-date clustering. Explicit state holidays, adjacent travel days, and school vacations do not explain the less restrictive regional gradients, but federal-state-by-date fixed effects materially change the comparison. Event-study, matched-event, and reconstructed nonavailability outcomes do not identify a clean average threshold-onset effect.

The adjustment diagnostics do not identify the mechanism behind the weaker downstream evidence. AIS crossing data show that persistent mixed-threshold low-navigation stress and selected high-water regimes are associated with lower realized tanker activity at affected gauge crossings. BASt road counts do not reveal a robust compensating increase in nearby truck traffic, and potential pipeline access and public supply-node measures do not establish systematic attenuation in retail-price gradients. Reconstructed availability, spatial price dispersion, time-weighted intraday variability, and event-based realized variation likewise yield no multiplicity-robust differential low-water effect. Taken together, the results document a coherent but inference-sensitive tanker-movement association, but neither a regional-control-robust scarcity gradient nor a measured domestic or cross-border buffer.

The added public-source evidence is heterogeneous. Several major petroleum ports show lower handling, but the aggregate import difference attenuates after year adjustment and observable terminal capacity does not produce a uniform attenuation pattern. The July 2026 holdout is best read as a negative-control case: most of the initial national price jump occurs before the official low-water gauge share rises sharply, while highly AIS-dependent grids do not exhibit a positive diesel premium. These diagnostics separate national co-movement, physical disruption, and regional pass-through without identifying a causal national price effect or a European trade buffer.

These findings are relevant for climate adaptation of transport infrastructure and for energy-market resilience. Hydrological extremes can be associated with freight disruption even when downstream retail-price responses are difficult to isolate; the current evidence does not establish a causal average increase in consumer fuel prices. The design does not identify structural transport-cost incidence, shipment-route elasticities, terminal inventories, pipeline off-take rights, or the marginal cost of barge capacity. It documents an asymmetry in the strength of the transport and retail evidence, not that observed supply-network buffers caused the weaker retail response.

The policy implication is narrower than a ranking of adaptation measures. The evidence shows that persistent low-water stress is associated with reduced tanker movement, while the analysis identifies neither a causal retail-price effect nor the mechanism limiting local pass-through. Resilience planning should therefore evaluate waterway operations and supply-chain contingency jointly. German policy already provides operational probabilistic water-level forecasts and is advancing targeted fairway optimization at Middle Rhine bottlenecks (Bundesministerium für Verkehr, 2024, 2025). The present results do not estimate the benefits of these measures, storage, terminal capacity, or modal substitution. Aggregate imports alone cannot establish a European buffer. Assessing these margins requires bilateral product flows and entry routes, terminal inventories and throughput, rail movements, and effective pipeline capacity linked to local prices.

Data availability

Analysis code, generated tables and figures, and a source-coverage manifest are available from the corresponding author during review and will be deposited in a public repository. Public inputs are documented with their provider and retrieval window. Licensed AIS records are not redistributed; qualified researchers must obtain access from the data provider.

Acknowledgements

We thank data providers and participants at the Economic Research Seminar at the University of Hohenheim, the 2025 Tübingen–Hohenheim Economics (THE) Young Researcher Workshop, and the 2026 Computational Science Hub (CSH) Young Researchers' Symposium on "Reproducibility in Science and Research" for helpful comments. All errors are our own.

Declaration of generative AI and AI-assisted technologies in the manuscript preparation process

The research design, initial analysis code, and initial manuscript drafts were developed by the authors before OpenAI Codex was introduced into the workflow. At a later stage, the authors used OpenAI Codex to assist with reviewing and revising analysis code and diagnostics, reproducibility checks, and manuscript language, organization, and submission materials. The authors reviewed and edited the AI-assisted output as needed and take full responsibility for the content of the publication.

References

Bedoya-Maya, F., Shobayo, P., Beckers, J., van Hassel, E., 2024. The impact of critical water levels on container inland waterway transport. Transp. Res. Part D Transp. Environ. 131, 104190. URL: https://doi.org/10.1016/j.trd.2024.104190, doi:10.1016/j.trd.2024.104190.

Bundesanstalt für Gewässerkunde (BfG), 2025. Einzugsgebietsgrenzen-DE. https://geoportal.bafg.de/smartfinderClient/?lang=de#/datasets/iso/c21d4842-39b0-469d-9828-956a583213e2. BfG Geoportal dataset. Accessed: 2025-06-24.

Bundesministerium für Verkehr, 2024. Statusbericht zum Masterplan Binnenschifffahrt. Official implementation report. URL: https://www.bmv.de/SharedDocs/DE/Anlage/WS/statusbericht-masterplan-binnenschifffahrt.pdf?__blob=publicationFile. status: August 2024; accessed July 20, 2026.

Bundesministerium für Verkehr, 2025. Planfeststellungsverfahren im Teilabschnitt 3 gestartet: Meilenstein am Mittelrhein. Press release 067/2025. URL: https://www.bmv.de/SharedDocs/DE/Pressemitteilungen/2025/067-schnieder-planfeststellung-mittelrhein.html. november 27, 2025; accessed July 20, 2026.

Christodoulou, A., Christidis, P., Bisselink, B., 2020. Forecasting the impacts of climate change on inland waterways. Transp. Res. Part D Transp. Environ. 82, 102159. URL: https://www.sciencedirect.com/science/article/pii/S136192091930149X, doi:10.1016/j.trd.2019.10.012.

European Commission, 2026. Weekly Oil Bulletin. https://energy.ec.europa.eu/data-and-analysis/weekly-oil-bulletin_en. Accessed: 2026-07-14.

Eurostat, 2025. Inland waterway transport statistics by product category. Technical Report. Statistical Office of the European Union. URL: https://ec.europa.eu/eurostat/statistics-explained/SEPDF/cache/31793.pdf. data extracted September 2024; accessed July 19, 2026.

Eurostat, 2026. Monthly Oil and Petroleum Products Statistics: Balances and Emergency Stocks. https://ec.europa.eu/eurostat/databrowser/explore/all/envir?lang=en&subtheme=nrg.nrg_quant.nrg_quanta.nrg_cb_oil&display=list&sort=category. Datasets nrg_cb_oilm and nrg_stk_oilm; accessed 2026-07-19.

Generaldirektion Wasserstraßen und Schifffahrt, 2023. FAQ: Niedrigwasser und Hochwasser in den Bundeswasserstraßen. URL: https://www.gdws.wsv.bund.de/SharedDocs/Kurzmeldungen/DE/20230717_Niedrigwasser_FAQ.html. published 17 July 2023; accessed 15 July 2026.

Horst, B., Müller, Y., 2025. Quantifying Waterway Supply Chain Shocks: Regional Propagation in the Rhine Area. URL: https://papers.ssrn.com/sol3/papers.cfm?abstract_id=4818090, doi:10.2139/ssrn.4818090. working paper, October 2025 version.

Jonkeren, O.E., Rietveld, P., van Ommeren, J.N., 2007. Climate Change and Inland Waterway Transport: Welfare Effects of Low Water Levels on the River Rhine. J. Transp. Econ. Policy 41, 387–411.

Pulido, J.M., Bedoya-Maya, F., van Hassel, E., Vanelslander, T., Carlan, V., 2025. Improving the visibility of waterway events influencing traffic along the Rhine, Main, and Danube. J. Transp. Geogr. 128, 104385. URL: https://doi.org/10.1016/j.jtrangeo.2025.104385, doi:10.1016/j.jtrangeo.2025.104385.

Statistische Ämter des Bundes und der Länder, 2026. Open Data der Binnenschifffahrtsstatistik 2011–2025. https://www.statistikportal.de/de/transport-und-verkehr/binnenschifffahrt. Port-to-port records by cargo category; accessed 2026-07-19.

Statistisches Bundesamt, 2023. Goods transport by inland waterways in 2022 at lowest level since German unification. Press release No. 119 of 27 March 2023, accessed: 2025-07-22.

tankerkoenig.de, 2025. Tankerkoenig.de Historical Fuel Price Data. https://dev.azure.com/tankerkoenig/_git/tankerkoenig-data. Data licensed under CC BY-NC-SA 4.0. Accessed: 24-06-2025. License: https://creativecommons.org/licenses/by-nc-sa/4.0/.

Unabhängiger Tanklagerverband e.V., 2025. Standorte und Kapazitäten der Mitgliedsfirmen. https://www.tanklagerverband.de/. Nameplate capacity as of 2025-01-01; accessed 2026-07-19.

Wasserstraßen- und Schifffahrtsverwaltung des Bundes (WSV), 2025. PegelOnline River Gauge Data. https://www.pegelonline.wsv.de. Observational data from PegelOnline; licensed under CC BY-NC-SA. Accessed: 2025-06-24.